Light-Controlled Conductance Switching of Ordered Metal-Molecule-Metal Devices

Molen, Sense Jan van der; Liao, Jianhui; Kudernac, Tibor; Agustsson, Jon S.; Bernard, Laetitia; Calame, Michel; Wees, Bart J. van; Feringa, Ben L.; Schönenberger, Christian

Published in:
Nano Letters

DOI:
10.1021/nl802487j

Publication date:
2009

Supporting Information

Light-controlled conductance switching of ordered metal-molecule-metal devices

S.J. van der Molen[*,1,2,3], J. Liao[1], T. Kudernac[4], J.S. Agustsson[1], L. Bernard[1], M. Calame[1], B.J. van Wees[2], B.L. Feringa[4], C. Schönenberger[1]

1: Department of Physics, University of Basel, Klingelbergstrasse 82, 4056 Basel, Switzerland

2: Physics of Nanodevices, Zernike Institute for Advanced Materials, University of Groningen, Nijenborgh 4, 9747 AG Groningen, The Netherlands

3: Kamerlingh Onnes Laboratorium, Leiden University, Niels Bohrweg 2, 2333 CA Leiden, The Netherlands

4: Stratingh Institute / Zernike Institute for Advanced Materials, University of Groningen, Nijenborgh 4, 9747 AG Groningen, The Netherlands

1. Details on sample preparation and experimental techniques

a) Sample preparation: We synthesize diarylethene molecules with two acetyl-protected thiol endgroups connected to the central switching unit via a metaphenyl spacer (Fig. 1a of the manuscript) [27,28]. Two-dimensional, hexagonally ordered arrays of octanemonothiol-covered nanoparticles are fabricated using the method described in Refs. 31 and 32. In the present study, two sample geometries are used. For the first type (including 'sample 1'), we stamp a large-scale array (≅ 4×4 mm), assembled on a water surface, onto a quartz substrate using a flat PDMS stamp. Next, we evaporate two gold contacts on top of the network, employing a thin Cu-wire as a shadow mask (45 nm Au / 5 nm Ti). Thus, the effective array size of 'sample 1' is relatively large (width: 3.14 mm, length: 200 μm). For the second type (including 'sample 2'), we use patterned PDMS stamps to transfer the self-assembled nanoparticle arrays. These stamps are prepared using standard UV-lithography to define narrow lines. Subsequently, we evaporate gold contacts using a TEM-grid as a shadow mask [31, 32]. The uncovered array on 'sample 2' has a width of 125 μm and a length of 8 μm. Molecular insertion is performed by immersing a sample in a 0.5 mM solution of the 'on'-state switch in tetrahydrofurane, for over 24 hours at 295 K. Finally, a sample is electrically contacted and inserted in an argon flow cell.

b) Experimental techniques: Optical absorption spectroscopy is performed with a halogen lamp and an Andor Shamrock 163i spectrograph connected to the side-port of an Olympus IX71 inverted microscope. For the experiments in Figs. 2 and 3 of the manuscript, a Labview routine is used. This program commences by measuring an I-V (current-voltage) curve ($-10<V<10V$) in the dark. Then, it opens a shutter for 5 seconds, during which the sample can be illuminated with the Hg-lamp, using different filters ('UV-filter': $300<\lambda<400$ nm; 'Vis-filter': $590<\lambda<650$ nm, or complete blocking). After the shutter is closed, the cycle is repeated. The conductance is measured exclusively in the dark to exclude photocurrents or heating effects. One cycle takes 26 seconds. Thus, real time in Figs. 2 and 3 of the manuscript is 26/5 times the illumination time.

2. Optical spectra of diarylethene molecules in solution

In Fig. S1, we show optical absorption spectra for thiolated metaphenyl-substituted diarylethene molecules in dry toluene. Figure S1a, displays the spectra for molecules in which the thiol group is 'protected' by an acetyl group. The closed, 'on'-state isomer (dashed red line) shows a broad absorption for $420 < \lambda < 630$ nm. Illumination at these wavelengths induces 'on' to 'off' switching. The open, 'off' isomer (solid black line) has only got absorption peaks in the UV region. Illumination with UV-light yields 'off' to 'on' switching.

In Fig. S1b, spectra are shown for thiolated metaphenyl-substituted diarylethene molecules bound (at one side) to small gold nanoparticles (2 nm in diameter) in dry toluene. Mie scattering on the nanoparticles clearly influences the absorption curves. Most notably, a small surface plasmon peak is present, as seen in the spectrum for the open molecules (black solid line, cf. Fig. S1a). However, the absorption peak of the closed diarylethene molecules (red, dashed line) still dominates the plasmon peak due to the small particle diameter. The ring-closure process is less efficient for molecules bound to nanoparticles (quantum yield: 7%) than for free molecules (quantum yield: 40%) (R. Hania *et al.* in preparation).

We note that for the 10-nm gold particles we use in 2D-arrays, the surface plasmon peak is strongly enhanced, as compared to the 2-nm ones in Fig. S1b. Therefore, the surface plasmon peak constitutes the main absorption peak around 600 nm. It dominates the typical absorption peak of the closed form molecules.

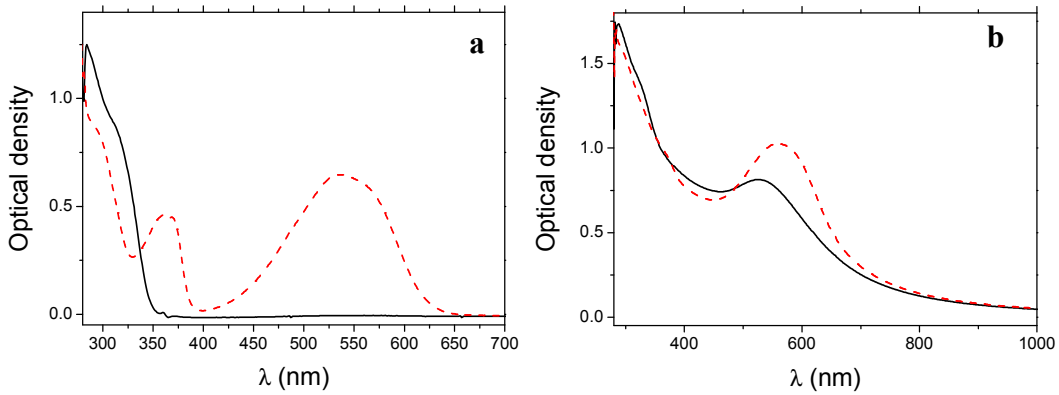

Figure S1 | a, **Optical absorption spectra of thiolated metaphenyl-substituted diarylethene molecules in dry toluene**. Black, solid line: open, 'off'- state molecule; red, dashed line: closed, 'on'-state molecule; note the broad absorption peak around 550 nm. **b**, Optical absorption spectra for the same molecules, after coupling to small gold nanoparticles. The nanoparticles induce Mie scattering. The surface plasmon peak is relatively weak, due to the small particle diameter (2 nm), so that the 'on'-state absorption peak dominates the spectrum of the closed molecules. For larger particles, as in the arrays, the surface plasmon peak dominates the spectrum.

3. Experiments in ambient conditions

Experiments in air at room temperature show reversible switching. However, switching is less pronounced than in an argon flow cell and the devices deteriorate faster. After 1 to 2 switching cycles the samples break down. An example is shown in Fig. S2, for a device of similar dimensions as 'sample 1' in Fig. 3 of the main manuscript (3.1x4.1 mm). We relate this to enhanced photodegradation effects during UV irradiation in air.

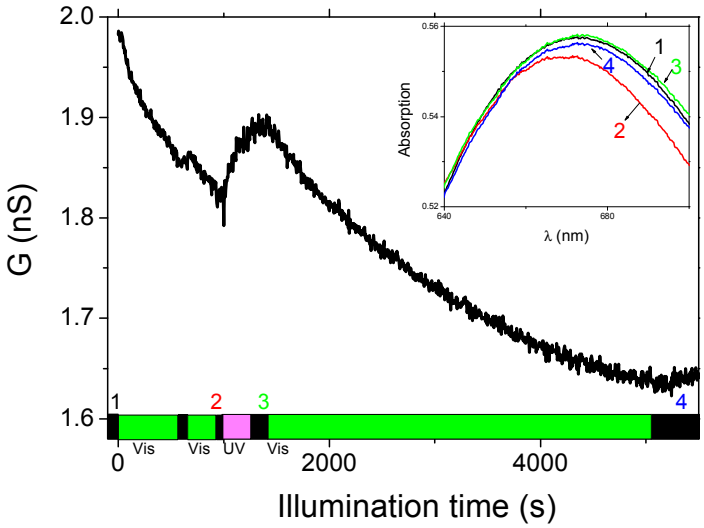

Figure S2 | Conductance and optical absorption experiments in ambient conditions. The device is similar to 'sample 1', length: 3.1 mm, width, 4.1 mm. First, at t<0, we take absorption spectrum 1 (see inset, using a halogen lamp). At t=0, we start irradiating the sample with visible light (see coloured bar; same 100 W Hg-lamp and filters as in Figs. 2 and 3 of the manuscript). This induces a conductance decrease, as seen in the main panel. We stop illumination for a short time around t=560 s, after which we proceed with visible illumination. Next, we stop illumination again and take spectrum 2 (inset). Clearly, the surface plasmon peak is blue shifted with respect to spectrum 1, demonstrating molecular 'on'-to-'off' conversion. Subsequently, we illuminate with UV-light (t=980 s). This results in a conductance increase. We stop UV-illumination and measure spectrum 3, which is very similar to spectrum 1. Finally, we irradiate with visible light again for an extended period. After this, we measure spectrum 4. The plasmon peak has moved to the red again, although the effect is limited now.

4. Photodegradation due to long UV-illumination in Ar flow cell

In Figure S3, we show an illumination experiment on a nanoparticle network with 'on'-state diarylethene bridges. The sample is similar to 'sample 1' in Figure 3 of the manuscript (length: 0.25 mm, width: 6.3 mm). The experiment is done in an argon flow cell, at room temperature. Visible illumination is started at t=0, resulting in a conductance decrease due to 'on' to 'off' switching. At t=245 s, we begin UV-irradiation. In contrast to Figures 2 and 3 of the manuscript, we use an extended UV-illumination time, which allows us to observe degradation effects. Just after UV-illumination has started, there is a steep conductance increase, which we relate to molecular 'on' to 'off' conversion. Some time later, the slope of the conductance curve decreases. We relate this effect to a competition of 'on' to 'off' conversion and irreversible reactions. Indeed, photodegradation is most pronounced for fully conjugated, 'on' state molecules, which are increasingly present during UV-irradiation. In this case, the extended UV-illumination led to failure of the sample. As shown in Fig. S3, the sample could not be switched a second time by illumination with visible light.

Interestingly, a similar change of slope during UV-irradiation can be seen in Figure 2 of the manuscript, although it is much less pronounced. By restricting UV irradiation, and hence limiting irreversible reactions, we were able to obtain 8 full switching cycles for 'sample 2'.

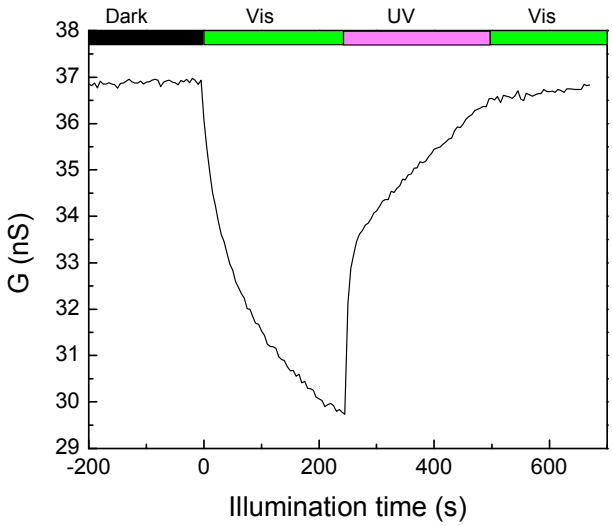

Figure S3 | Illumination experiment on a network with 'on'-state bridges. At t=0, illumination with visible light is started. At t=245 s, long-term UV irradiation begins (see coloured bar at top). This leads to a competition of 'on'-to-'off' conversion and photodegradation effects. Subsequent illumination with visible light has no effect on the conductance.

5. Illumination of octanemonothiol-covered nanoparticle networks

We performed reference experiments on octanemonothiol-covered nanoparticle networks. These are samples as prepared *before* molecular bridging, of similar dimensions as 'sample 2' considered in Figure 2 of the main manuscript (length: 10 μm, width: 230 μm). Figure S4a shows the influence of illumination on the conductance of such a sample (Argon flow cell, room temperature). The conductance G(t) has been normalized to its initial, low value G(t=0)=0.496 nS. This allows for a comparison with 'sample 2' and Fig. 2 of the main manuscript (replotted in Fig. S4b, after normalization). Visible light is found to have little effect on the octanemonothiol device: conductance changes are small and can go either way. UV illumination, on the other hand, induces a small conductance *decrease* in the first run. We relate this to photodegradation effects, possibly of the Au-S bond in the monothiol molecules.

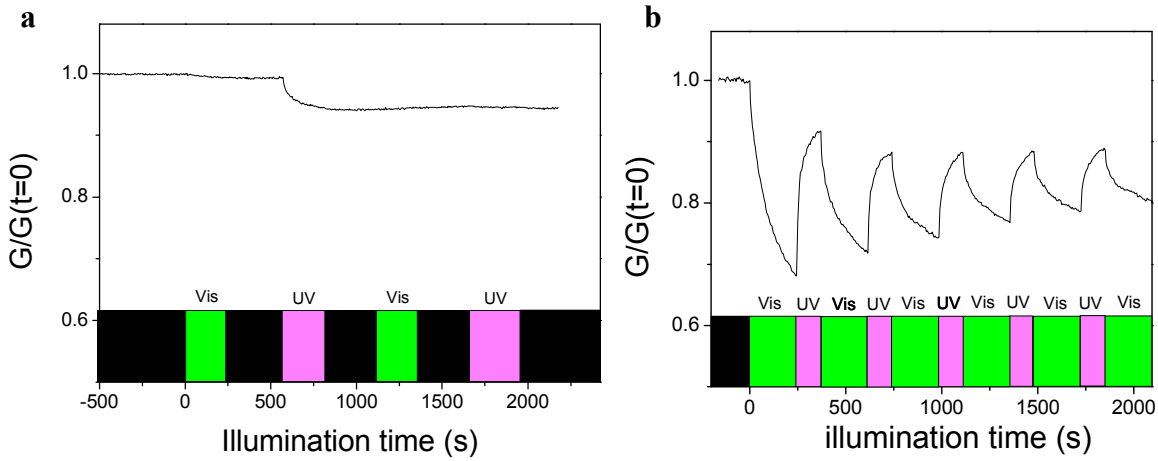

Figure S4 | a, Conductance evolution during illumination for a network of octanemonothiol-covered nanoparticles. The conductance is normalized to G(t=0) = 0.496 nS. For t<0, the sample is in the dark. Illumination with visible light is started at t=0, followed by a period in the dark, by UV-illumination etc. **b,** First five switching events for 'sample 2' (see Fig. 2, main manuscript). Also here we normalized the conductance.

6. Illumination of nanoparticle networks bridged by OPV-dithiol molecules

We performed reference experiments on nanoparticle networks, in which (oligo(=3)-phenylenevinylene-dithiol molecules (OPV) have formed bridges between neighbouring nanoparticles (see Fig. S5a). These samples are of similar dimensions as 'sample 2' considered in Figure 2 of the main manuscript (length: 10 μm, width: 150 μm)**.** Figure S5b shows the evolution of the conductance during illumination (Argon flow cell, room temperature). The conductance values have been normalized to the initial conductance G(t=0)=50.6 nS. This allows for a comparison to 'sample 2' and Fig. 2 of the main manuscript (replotted in Fig. S5c, after normalization). Indeed, for the OPV sample, the overall conductance variations are small. In the dark, the sample conductance increases somewhat, giving rise to a small background slope. Visible light is found to have virtually no effect on the device. UV illumination gives rise to a slight *decrease* of the conductance. This is consistent with photodegradation effects, taking place under UV irradiation. Note the pronounced difference with the data on the diarylethene switches, Figs. 2 and S5c, where UV irradiation gives rise to a large conductance *increase*.

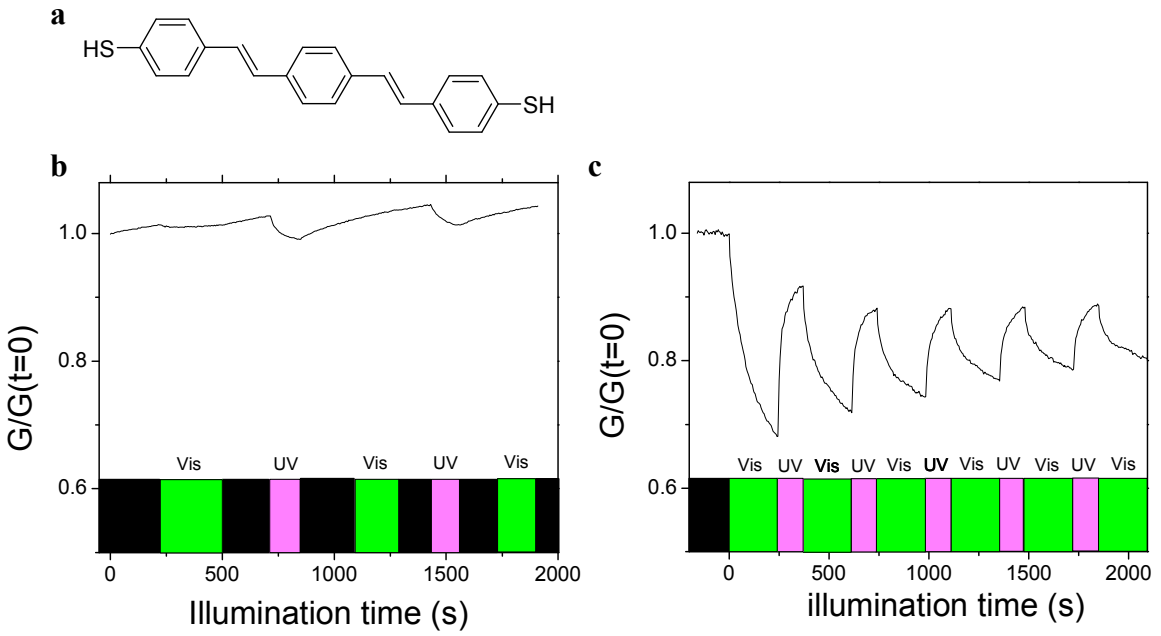

Figure S5 | Conductance evolution (b) during illumination for a network of nanoparticles, bridged by OPV-dithiol molecules (drawn in a). The conductance is normalized to G(t=0) = 50.6 nS. For t<0, the sample is in the dark. Illumination with visible light is started at t=0, followed by a period in the dark, by UV-illumination etc. **c,** First five switching events for 'sample 2' (see Fig. 2, main manuscript). Also here we normalized the conductance.

7. Scanning electron microscopy

In Fig. S6, we show a scanning electron microscopy (SEM) image of 'sample 1' taken after the experiment shown in Figure 3 of the manuscript. The nanoparticle structure is still intact. Moreover, neither visible nor UV-illumination has changed the nanoparticle lattice. Hence, structural changes during illumination cannot explain the data in Figure 3.

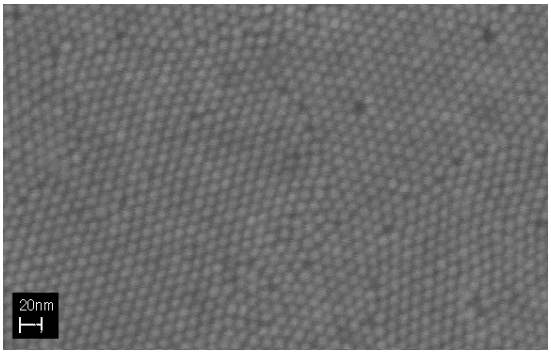

Figure S6 | Scanning electron micrograph of 'sample 1'. The image was taken after the experiment displayed in Figure 3 of the manuscript. The nanoparticle lattice structure has not been influenced by visible nor by UV illumination.

8. Percolation

Here, we employ percolation theory to model the conductance for 'sample 2' after sequential visible and UV illumination (see Fig. 2 of manuscript). Our calculation is based on the general effective medium equation, which has proven to give a successful relation between conductance, G, and the percentage of neighbouring nanoparticle pairs that are bridged by closed, 'on'-state molecules, p [36, 37]. For a 2D-system, it reads:

$$\frac{(1-p)(G_0^{3/4}-G^{3/4})}{G_0^{3/4}+A_c G^{3/4}}+\frac{p(G_1^{3/4}-G^{3/4})}{G_1^{3/4}+A_c G^{3/4}}=0 \qquad (1)$$

where G_1 is the conductance of the sample if all nanoparticle pairs are bridged by closed, 'on'-state molecules, i.e., $G_1=G(p=1)$. Equivalently, G_0 is the conductance of the sample if all nanoparticle pairs are bridged by open, 'off'-state molecules, i.e., $G_0=G(p=0)$. We take $G_1 = 25\ G_0$. The constant $A_c=(1-p_c)/p_c=1.88$ is related to the percolation threshold, $p_c=2\sin(\pi/18)=0.35$, for a triangular, 2D network.

We assume that at t=0 all nanoparticle pairs are bridged by closed, 'on'-state switches, i.e. $p(t=0)=1$ so that $G_1=3.2$ nS (see Fig. 2). After the first illumination with visible light (defined as t=1/2, i.e., half an illumination period), a fraction x of the closed molecules will have switched open, i.e., $p(t=1/2)=1-x$. After subsequent UV illumination (defining t=1), a fraction y of the open molecules will have switched back, etc. Figure S7 shows the conductance for the 2D-network after each illumination step, calculated using eq. (1). To fit the first points of Fig. 2 in the manuscript, we need x=0.2 and y=0.7. As seen in Fig. S7, two 'photostationary states' come about, partly explaining the decay in Fig. 2. The additional decay observed in Fig. 2 is therefore related to photodegradation effects.

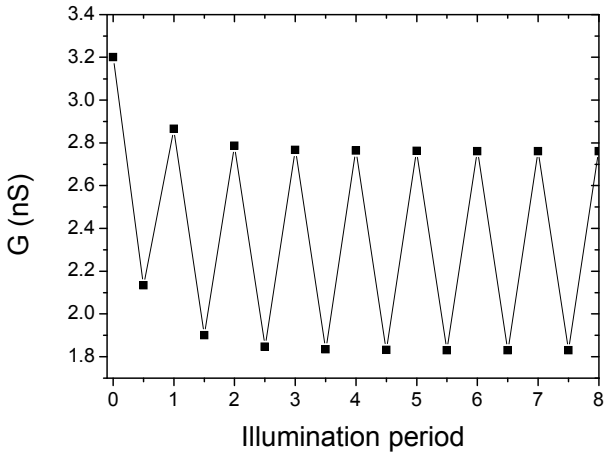

Figure S7 | Calculation of sample conductance using a percolation model. The initial conductance is based on 'sample 2'. With time, two photostationary states appear, partly explaining the decay in Fig. 2 of the manuscript. Note that the time axis is defined in periods. After each full period of visible and UV illumination, t=n is integer. After visible illumination, t = n+1/2

References (numbering is the same as in the main manuscript)

[27] Kudernac, T., de Jong, J.J., van Esch, J., Feringa, B.L., Dulic, D., van der Molen, S.J., van Wees, B.J. *Mol. Cryst Liq. Cryst*. **430**, 205-210 (2005);

[28] Kudernac, T., van der Molen, S.J., van Wees, B.J., Feringa, B.L.
Chem. Comm. 3597-3599 (2006)

[31] Liao, J., Bernard, L., Langer, M., Schönenberger, C.; Calame, M.
Adv. Mater. **18**, 2444-2447 (2006)

[32] Bernard, L., Kamdzhilov, Y., Calame, M., van der Molen, S.J., Liao, J., Schönenberger, C.
J. Phys. Chem. C **111**, 18445-18450 (2007)

[36] Kirkpatrick, S.,
Rev. Mod. Phys. **45**, 574-588 (1973)

Additional Reference:

[37] Wu, J.; McLachlan, D.S.
Phys. Rev. B **56**, 1236-1248 (1997)